IPPI

Polyolefins Journal, Vol. 7, No. 1 (2020)
DOI: 10.22063/poj.2019.2447.1132

ORIGINAL PAPER

Interplay of reversible chain transfer and comonomer incorporation reactions in coordination copolymerization of ethylene/1–hexene

Ali Ebrahimi[1], Saeid Ahmadjo[2], Mohsen Mohammadi[3], Mohammad Mahdi Mortazavi[2], Mostafa Ahmadi[1,4*]

[1]Department of Polymer Engineering and Color Technology, Amirkabir University of Technology, Tehran, Iran
[2]Engineering Department, Catalyst Group, Iran Polymer and Petrochemical Institute, Tehran, Iran
[3]Department of Polymer Engineering, Faculty of Engineering, Qom University of Technology, Qom, Iran
[4]Institute of Physical Chemistry, Johannes Gutenberg-Universität Mainz, Duesbergweg 10-14, D-55128 Mainz, Germany

Received: 16 April 2019, Accepted: 10 June 2019

ABSTRACT

Coordinative chain transfer polymerization (CCTP) has opened a new path for the development of novel products like olefin block copolymers and chain-end functional polyolefins. However, conflicting results are frequently reported on the catalyst performance including activity and comonomer selectivity under CCTP conditions. Here we have selected two catalysts including rac-ethylenebis(1-η^5-indenyl)zirconocene and bis(imino)pyridine iron, with drastically different comonomer affinities. The effect of diethyl zinc as the chain transfer agent (CTA) on their individual performances is evaluated at different 1–hexene concentrations, in copolymerization with ethylene. Combined thermal fractionation and GPC results confirm that not all chains experience the reversible transfer reaction. Nevertheless, the metallocene catalyst shows twice activity and about 30% lower comonomer incorporation in the presence of CTA. Conversely, the late transition metal catalyst demonstrates lower activity and remains comonomer irresponsive. It could be concluded that, in addition to establishing a reversible transfer reaction, CTA affects the nature of active centers. This finding can help designing olefin copolymers with a more defined chemical composition based on CCTP reaction. **Polyolefins J (2020) 7: 1-11**

Keywords: Coordination polymerization; reversible chain transfer reaction; chemical composition; microstructure.

INTRODUCTION

Precise control of the chain microstructure has been an enduring goal in polymerization reaction engineering. Key microstructural features of the copolymers, including the molar mass and branching and more specifically chemical composition and their distributions, can be ideally controlled in living polymerization systems. In the last two decades, the living reaction characteristics have been introduced in the coordination polymerization techniques based on different mechanisms [1, 2].

The catalyzed chain growth is a living coordination polymerization method, which is based on the reversible transfer of the growing chains to a dormant state. In this mechanism, the majority of polymer chains reside on an inexpensive main-group metal and are not able to grow unless reversibly transferred to the transition metal catalyst [3, 4]. For instance, bis(imino)pyridine iron

---

* Corresponding Author - E-mail: mo.ahmadi@aut.ac.ir

complex is shown to perform catalyzed chain growth of ethylene on diethyl zinc as the reversible chain transfer agent (CTA) [5, 6]. Consequently, a Poisson distribution of chain length was achieved by fast and reversible transfer of growing chains between iron and zinc metal centers [5]. New olefin block copolymers (OBCs) were introduced, on the basis of this reaction, by simultaneous application of two catalysts with drastically different comonomer affinities in copolymerization of ethylene and 1–octane [7, 8]. In this reaction pathway, a growing chain has the chance to be transferred to the CTA and to be cross-shuttled to the other catalyst and produce segments with different comonomer contents (note that shuttling back to the same catalyst just extends the length of the current block). Therefore, such OBCs are composed of crystalline polyethylene block and amorphous copolymer segments [9-13]. The other notable outcome of the catalyzed chain growth is the synthesis of chain-end functional polyolefins. The highly reactive alkyl–metal bond at the chain end can be transformed into different functionalities, to provide olefinic building blocks for the production of block copolymers [14-16].

Unfortunately, not all transition metal catalysts can perform catalyzed chain growth in combination with every main-group metal alkyl [6, 17]. For instance, replacing the alkyl groups of diethyl zinc with methyl, in combination with bis(imino)pyridine iron complex, leads to a broader distribution of chain lengths, and the use of bulkier groups like tolyl or phenyl shows evidences of irreversible chain transfer, and even no chain transfer reactions, respectively [6]. The difficulty encountered in finding a good match between polymerization catalysts and CTAs has hampered development of OBCs based on new catalytic systems [7]. Only some general guidelines can be drawn for finding the matched catalytic systems, based on the limited available experimental data and theoretical investigations [7, 17-19]. However, even in such matched systems, still much less is known about the effect of reversible chain transfer reaction on the distinct performance of catalysts [20, 21]. The situation is even more complicated for the production of OBCs in the presence of two different catalysts [3, 6, 17, 22, 23]. The complication is amplified in batch reaction conditions, where the relatively different consumption rates of the two catalysts alter the instantaneous feed composition, as well [24-26]. However, the available kinetic models for individuall [24, 27] or binary [10, 11, 25, 28, 29] catalytic systems are built based on the independent performance of individual catalysts in the absence of CTA, which of course results in discrepancies between the predictions and the experimental data [17, 30]

Using the terminal model, Zhang et al. have shown that the presence of CTA has no impact on the composition of active centers in a single catalyst copolymerization reaction, and thus, Mayo–Lewis equation is valid [28]. However, experimental records from ethylene/norbornene [31] and styrene/isoprene [32-34] coordinative chain transfer copolymerizations (CCTP) have shown that depending on the utilized catalytic system, introducing CTA can significantly affect the chemical composition of the final product [35]. The outcome of CCTP using a binary catalytic system cannot be predicted on the basis of their individual performances, likewise. Surprisingly, copolymerization of styrene/isoprene, in a binary catalytic system, has revealed that incorporation of styrene is significantly higher, both in the hard and in the soft blocks, compared to the case where single catalysts are used at the same feed composition [36].

Consequently, deviations from the theoretical expectations mainly stem from the modifications of the polymerization catalyst in presence of CTA and not from kinetic aspects. There are limited studies that highlight and explain such inconsistencies [20]. Specifically, reports on the interplay of reversible chain transfer reaction and the comonomer selectivity of the catalysts in olefin copolymerization are limited [18]. In this work, we have selected two catalysts with remarkably different comonomer affinities and studied their performances in the presence of varying amounts of CTA. Our results confirm that CTA indeed affects catalyst performances in terms of activity and comonomer selectivity, but to different extents.

EXPERIMENTAL

Materials

Methylaluminoxane (MAO, 10 wt% solution in toluene), diethylzinc solution ($ZnEt_2$, 1 M in hexane), and ansa-ethylenebis(1-η^5-indenyl)zirconium dichloride (Scheme 1a) are purchased from Sigma-Aldrich. Aniline is purchased from Merck and vacuum distilled before use. 2,6-Diacetylpyridine (purity>99%) is prepared from Acros. The bis(imino)pyridine iron complex (Scheme 1b) is synthesized according to the previous reports [37]. Toluene is refluxed and distilled over sodium wire before use and kept over 4Å/13X activated molecular sieves.

Polymerization

Ethylene/1–hexene copolymerization reactions are conducted in a 200 mL stainless steel Buchi reactor, using toluene as the solvent. The reactor is purged with nitrogen at 90°C for 2 hours prior to each reaction. Dried toluene and predetermined amount of comonomer are introduced under nitrogen atmosphere, and catalyst system is transferred in the following order: MAO is introduced as the main scavenger and cocatalyst, followed by $ZnEt_2$ as CTA, if needed, and finally the catalyst solution is injected via a syringe. The reactor is saturated with ethylene to the desired pressure, and the reaction starts and proceeds for 30 minutes by mixing. Ethylene consumption is compensated using a mass flow meter to keep the pressure constant and the consumption rate is recorded. Finally, the reactor is evacuated, and the product is precipitated in acidic methanol and vacuum dried.

Characterization

High temperature Gel Permeation Chromatography (GPC, PL-220) coupled with two refractive index and light scattering detectors, is used for determination of molar mass distributions (MMDs) using 1,2,4-trichlorobenzene at 150°C as solvent flowing at the rate of 1 mL min^{-1}. A universal calibration curve is constructed using 12 standard polystyrene samples (PL) covering molar mass range of 1×10^3-6×10^6 g mol^{-1} to determine the average molecular weights and polydispersity indices (PDI).

Differential Scanning Calorimetry (DSC) is carried out using Mettler-Toledo apparatus 823e Module, interfaced to Star E 9.01 software (sensor FRS5) at the rate of 10°C min^{-1}. Samples are heated from room temperature to 160°C and remained for 10 min for erasing the thermal history, followed by cooling to 0°C and heating to 160°C using the same rate. Melting temperature and crystallinities are recorded according to the results of the final step.

Successive Self-nucleation and Annealing (SSA) analysis is performed on the same DSC apparatus at the rate of 10°C min^{-1}. Samples are first heated to 160°C, maintained for 10 min, and cooled to 25°C. Subsequently, samples are heated to the first self-nucleation temperature (Ts_1, 145°C), kept for 10 min, and cooled down to 25°C. The successive self-nucleation is achieved by repeatedly heating to the next self-nucleation temperature steps, and cooling to 25°C. The temperatures were 6°C distant from each other. After covering the temperature range between 145 and 38°C, the final heating ramp from 25 up to 160°C is applied to collect all melting endotherms.

^{13}C NMR measurements are carried out by dissolving about 80 mg of polymer in 0.7 mL of benzene-d6 and 1,3,5-trichlorobenzene (20% v/v). The spectra are recorded using Bruker NMR AVANCE400 spectrometer operating at 100°C, and methylene sequences chemical shift in 30.00 ppm is used as the internal chemical shift reference. The applied measurement conditions are as follows: 5 mm probe, 90˚ pulse angle, acquisition time 1.5 s, delay time 4.0 s, about 17000 scans or 5 hours measurement.

RESULTS AND DISCUSSION

Our investigation is based on two sets of ethylene/1–hexene copolymerization reactions, using two different catalysts, at varying levels of 1–hexene feed ratios. We have chosen catalysts with remarkably different comonomer affinities. Both catalysts are already proven to be capable of performing catalyzed chain growth in combination with $ZnEt_2$ [5, 6, 17, 38]. Therefore, they have the potential to be used together in a binary catalytic system for production of new block copolymers. Accordingly, we have utilized similar reaction conditions, which simplify the comparison of their individual performances and provide more insights for studying their simultaneous application.

The first catalyst, rac-ethylene bis(1-η^5-indenyl)zirconium dichloride metallocene (Scheme 1a), hereafter named Zr catalyst, is distinguished for the formation of linear polyethylene chains in a CCTP reaction [17]. Due to the presence of the ethylene bridge, this catalyst has an open angle for the incorporation of comonomers like α-olefins [39]. The second late transition metal catalyst, bis(imino)pyridine iron dichloride (Scheme 1b), hereafter named Fe catalyst, can afford linear polyethylene chains with broad molar mass distribution, comparable to Ziegler-Natta catalysts [40]. The presence of bulky substitutes on the ortho-position of the aryl groups locks them orthogonal to the N-N-N plane, and decreases the frequency of chain transfer reactions, which leads to a high molar mass [41]. Due to the aforementioned planar structure, this catalyst has a very low tendency to incorporate bulky comonomers [41].

In the utilized reaction conditions, both catalysts have reported to provide chains with lower molar mass and PDI values in the presence of $ZnEt_2$ [5, 6, 17]. However, the effects of CTA on the comonomer selectivity of the catalysts are not studied. This unseen factor is very important in designing OBCs, which are produced by simultaneous application of two catalysts with different comonomer affinities. Since, the most important properties of OBCs are governed by their blocks compositions. For instance, the difference in the comonomer content of hard and soft blocks determines the crystallization kinetics and the extent of mesophase separation [12, 13, 42]. Therefore, in this study, we focus on the effect of CTA on the comonomer selectivity of two catalysts with drastically different comonomer selectivity, in separate reactions.

It is necessary to use the highest reaction temperature to dissolve the growing chains in the reaction medium and establish an effective reversible transfer reaction [16]. Both catalysts have already shown living reaction features at room temperature [5, 6, 17, 38]. We further increase the reaction temperature to 50°C to prolong the extent of reversible chain transfer reaction and still have adequate reactivity for both catalysts. Higher reaction temperature is favored for the Zr catalyst; however, it significantly hampers the activity of the Fe catalyst [41, 43]. The synthesized samples and other reaction conditions are explained in Table 1.

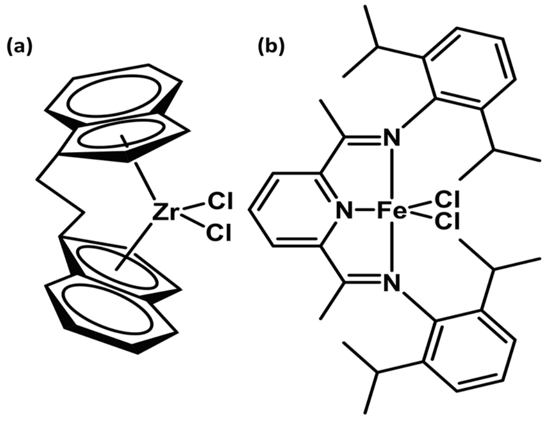

Scheme 1. Structure of the utilized catalysts: (a) rac-ethylenebis(1-η^5-Indenyl)zirconium dichloride and (b) bis(imino)pyridine iron dichloride.

Samples are coded as “CatXHY”, where Cat takes Zr or Fe, X stands for the [CTA]/[Cat] molar ratio and Y determines the amount of utilized 1–hexene comonomer in mL. After preliminary tests to find the overlap of the best operating conditions for both catalysts, the effect of [CTA]/[Cat] molar ratio and comonomer content is studied as outlined in Table 1.

The reaction yield is one of the most important practical properties of a catalytic system. The effect of reactant concentrations on the catalytic activities of the Zr and Fe catalysts are displayed in Figure 1. The activity of the metallocene catalyst increases by both the comonomer and the CTA concentrations (main plot, check Run 9 in Table 1 for the effect of CTA concentration, which is not shown in Figure 1). The amplification of the catalyst activity in ethylene polymerization upon introduction of different α-olefin comonomers, has been frequently attributed to the reduction in the formation of the relatively stable metal–ethyl intermediate [44-46]. The introduction of $ZnEt_2$ in ethylene/1–hexene copolymerization, using the same Zr catalyst, has been reported to result in a two-fold increase of catalyst activity, in agreement with our results [47]. $ZnEt_2$ is very reactive towards electron donating compounds like moisture, O_2 or CO_2. The increase in activity can be therefore due to the scavenging effect of the CTA, but the exact reason is not clear.

Conversely, the activity of the Fe catalyst decreases both by the comonomer concentration and by the introduction of CTA (inset plot, check Run 16 in Table 1 for the effect of CTA concentration, which is not shown in Figure 1). By introduction of the comonomer, the relative concentration of monomer decreases in the reac-

Table 1. Concentration of the components in ethylene/1–hexene copolymerizations using the individual catalyst systems and the corresponding activities and thermal properties.

Run	Code	Cat	[CTA]/[Cat]	1–hexene (mL)	Activity×10^{-6} (gPE $[Cat]^{-1}$ atm^{-1} h^{-1})	Tm (°C)	Xc (%)
1	Zr0H0	Zr	0	0	774	133	59.1
2	Zr0H3	Zr	0	3	1190	-	9.5
3	Zr0H6	Zr	0	6	1812	-	1.9
4	Zr0H12	Zr	0	12	2137	-	0.9
5	Zr550H0	Zr	550	0	1979	132.5	72.1
6	Zr550H3	Zr	550	3	2935	102.7,114.4	46.4
7	Zr550H6	Zr	550	6	3640	98.4	36
8	Zr550H12	Zr	550	12	4356	110.4,116.2	2.9
9	Zr100H3	Zr	100	3	2650	nd	nd
10	Fe0H0	Fe	0	0	667	133.2	75.4
11	Fe0H3	Fe	0	3	476	133	69.9
12	Fe0H6	Fe	0	6	420	134.56	70.7
13	Fe100H0	Fe	100	0	184	113.5,126.5	48.7
14	Fe100H3	Fe	100	3	257	106.3,126.8	47.3
15	Fe100H6	Fe	100	6	300	102.3,125.8	55.8
16	Fe550H3	Fe	550	3	130	nd	nd

Polymerization conditions: [Catalyst]= 3 μmol, Temperature: 50°C, Polymerization time: 30 min, Solvent: 80 mL of Toluene, Ethylene pressure: 2 bar, [MAO]/[Cat]= 1000.

tion medium, and since the Fe catalyst has no reactivity towards the 1–hexene; the overall yield decreases at higher comonomer levels. Decrease of catalyst activity in presence of CTA could be related to the excessive complexation of main-group metal and formation of relatively stable bimetallic complex with the catalyst. These stable species have low tendency toward the reverse de-complexation from the active center and therefore reduce the chain growth [3, 6, 47]

Comonomer incorporation has a drastic effect on the thermal properties of ethylene/α-olefin copolymers [48]. The melting temperature and the extent of crystallinity are decreasing functions of the comonomer content [49]. These longstanding correlations have been frequently used for indirect determination of comonomer content based on thermal properties of different ethylene/α-olefin random copolymers [48]. In this study, the crystallization decreases at higher comonomer concentrations, and by introduction of CTA, for the case of comonomer selective, Zr catalyst, as listed in Table 1. Figures 2a shows the corresponding melting endotherms before (main plot) and after (inset plot) the introduction of CTA. The ethylene homopolymer has a sharp melting peak above 130°C, while the random copolymers have broad melting peaks spreading from 40 to 80°C. The broad and weak peaks of random copolymers turn into noticeable bimodal peaks, and shift to higher temperatures, in presence of CTA. It could be qualitatively implied that CTA significantly reduces the comonomer selectivity of the Zr catalyst. However, the bimodality of the melting peaks says that this effect is not similar for all chains. The obtained product is in fact a blend of random copolymers with different chemical compositions. In the case of the Fe catalyst, however, the extent of crystallinity does not depend on the comonomer concentration, with or without CTA, as listed in Table 1. All melting

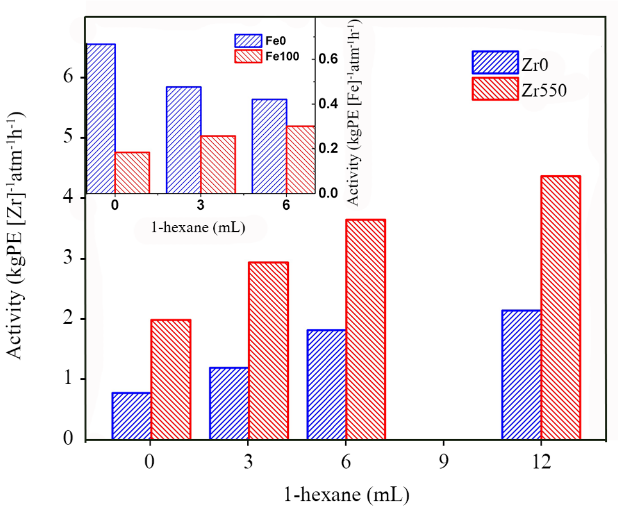

Figure 1. Effect of 1–hexene concentration on the activity, with and without CTA, for the Zr catalyst (main plot) and the Fe catalyst (inset plot). Polymerization conditions: [Catalyst]= 3 μmol, temperature: 50°C, reaction time: 30 min, solvent: toluene (80 mL), ethylene pressure: 2 bar, [MAO]/[Cat]= 1000.

endotherms show a sharp peak above 130°C, in the absence of CTA, as shown in Figure 2b. On contrary, a second low-temperature peak appears upon introduction of CTA, even in the absence of any comonomer. The appearance of low temperature endotherm in the absence of comonomer could be related to the excessive transfer to CTA and formation of low-molar mass chains. These chains are very short, [5, 43, 50] and therefore they have larger crystallization rate.

Successive Self-nucleation Analysis (SSA) is developed for segregation of ethylene/α-olefin copolymers, based on their comonomer content, by isothermal annealing. It has been widely used as a quantitative alternative for NMR and TREF, for determination of comonomer content [51-53]. SSA fractionation of the copolymers made at similar feed composition in presence and absence of CTA are compared for both catalysts in Figure 3. The fractionated peaks are deconvoluted based on the weighted summation of several Gaussian distributions. Details of the deconvolution method can be found elsewhere [48]. Sample Zr0H3, has several low-temperature melting peaks, due to the broad ethylene sequence lengths, as shown in Figure 3a (main plot). Such short ethylene sequences have little crystallization tendencies, and therefore, the sharp peaks appearing in this region represent a significant fraction of chains. This is quantitatively taken into account by normalizing the peak intensities with the crystallinity at each temperature step. According to Hosoda's equations for melting temperature and crystallinity of ethylene/1–hexene copolymers [49], this sample contains 14.7 wt% of comonomer with dispersity index of 1.07 [48]. The low-temperature peaks significantly diminish upon the introduction of CTA, in sample Zr550H3, and new peaks appear around 100°C (inset plot). The calculated average comonomer content is around 8.3 wt% with dispersity index of 1.28. Therefore, the introduction of CTA has decreased the comonomer content more than 30%, and increased the heterogeneity of comonomer distribution to the same extent. The broadening of comonomer distribution implies that not all chains are similarly affected by the presence of CTA, as expected.

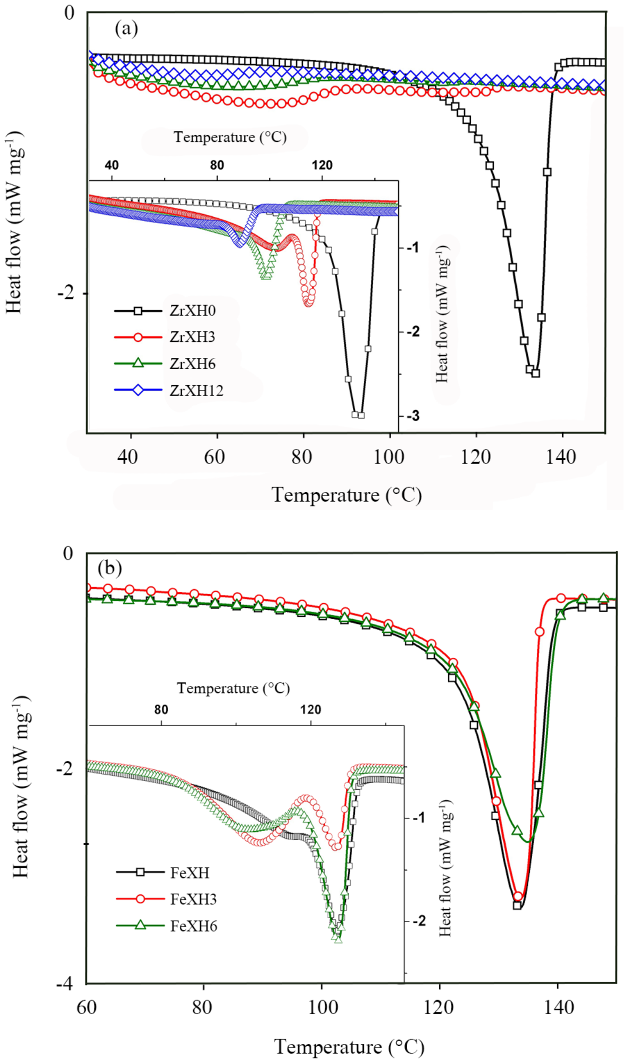

Figure 2. Effect of comonomer concentration on the melting endotherms of the copolymers made by the Zr catalyst (a) and the Fe catalyst (b) without (main plots) and with (inset plots) CTA.

On contrary, the SSA fractionation of Fe0H3 sample offers narrow melting peaks overlapping specially above 120°C. The calculated average comonomer content is not more than 1.3 wt%, which is below the sensitivity of such indirect method [48]. The introduction of CTA, in sample Fe100H3, provides broad melting peaks below 120°C. These peaks could be originated from high comonomer incorporation, if the average molar mass was not drastically altered. However, Fe catalysts are prone to have multiple active centers, which respond differently to the presence of CTA [43, 50, 54]. Therefore, the formation of low-molar mass chains due to excessive transfer to CTA is responsible for the low-temperature melting peaks, as follows.

As already explained, the decrease in molar mass and PDI values has been traditionally used as a signature of living polymerization behavior. However,

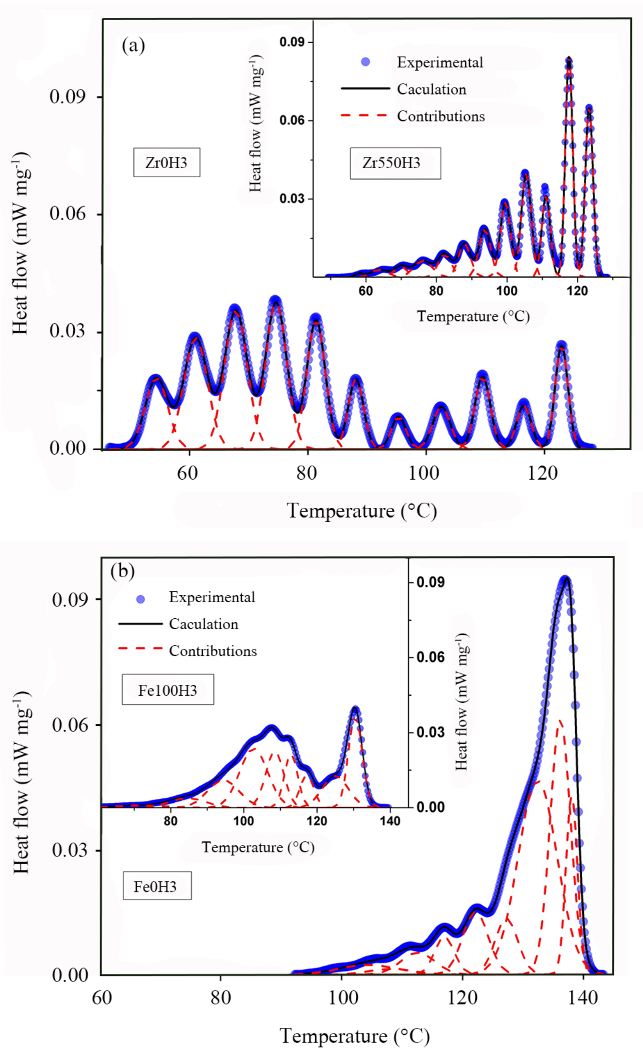

Figure 3. SSA fractionation of copolymers made by the Zr catalyst (a: Zr0H3 and Zr550H3) and the Fe catalyst (b: Fe0H3 and Fe100H3) without (main plots) and with (inset plots) CTA.

Hustad and coworkers have shown that the end-of-batch molar mass data cannot approve the living polymerization features, and the evolution of molar mass distribution during CCTP should be the basis of the judgement [25, 27]. They simply said, despite reversibility of the transfer reaction, high PDI values are often obtained if the relative propagation and transfer rates are not optimized [27].

Accordingly, the molar mass distributions of the two copolymers made in presence and absence of CTA are compared for both catalysts in Figure 4. The Zr catalyst shows about one decade decrease in molar mass upon introduction of CTA. However, in contrast to the expectations, the polydispersity index (PDI) increases from 2.11 to 2.6. Such PDI values are frequently reported for metallocene-catalyzed polymerizations in batch conditions, and the ideal PDI value of 2 is rarely encountered [46]. Conversely, the Fe catalyst has a broad and bimodal MMD in the absence of CTA, in accordance with the previous reports [5, 50, 54]. The broad MMD has been attributed to presence of more than one active center [54]. Clearly, the molar mass of both polymer fractions decreases by the introduction of CTA, but to a different extent. The formation of the low-molar mass fraction is responsible for the appearance of low-temperature melting endotherms in Figure 3b. The GPC data, therefore, imply the establishment of a quasi-living polymerization, in agreement with SSA data. Simply put, at the utilized conditions, just a fraction of chains finds the chance to experience the reversible chain transfer reaction. Nevertheless, this fraction causes lower comonomer content and higher activity, for the case of Zr catalyst. Consequently, the effect of CTA on comonomer selectivity should be stronger at the optimized reaction conditions.

The thermal fractionation data, as shown in Figure 3, are contaminated with excessive formation of low-molar mass chains, specifically in the case of the Fe catalyst. To decouple the effect of comonomer incorporation from molar mass, the ^{13}C NMR spectra of the samples are compared in Figures 5. The samples made by the Zr catalyst, especially in presence of CTA, provide higher intensities due to better solubility at the measurement conditions. The peak at 14 ppm reflects the methyl groups residing both at the end of the chain

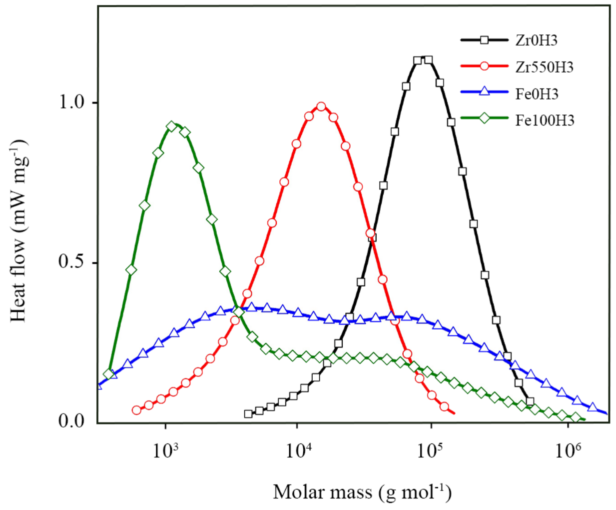

Figure 4. Effect of CTA on the molar mass distribution of copolymers made by the Zr and Fe catalysts with and without CTA.

and at the end of the butyl pendant groups of the comonomer units. The chemical shift at 38 ppm only denotes the tertiary carbon atom at the branch junctions. According to the obtained results, the comonomer content of the copolymers made by the Zr catalyst decreases from 12.54 wt% to 9.55 wt%, in presence of CTA. Consequently, steric hindrance due to the frequent complexation of CTA affects the incorporation of bulkier comonomer more significantly. Evidently, the polymers produced by the Fe catalyst do not contain any 1–hexene units, in the presence or the absence of CTA. Therefore, the low-molar mass fraction of polymers made in presence of CTA is responsible for the low-temperature melting peaks, regardless of comonomer concentration.

Our results clearly suggest that CTA can affect the chemical composition in a CCTP reaction. In the classical free radical copolymerization, the chemical composition is determined based on the reactivity ratios. Reactivity ratios are determined from homo- vs co-polymerization rate constants of each monomer. In a simple radical copolymerization, rate constants mostly depend on temperature. CTAs only regulate the chain length and do not compete with monomer incorporation and therefore cannot change the chemical composition. In coordination copolymerization, however, rate constants also depend on the type of the utilized catalyst. The CTA may not compete with monomer insertion reaction, but it can affect the active catalyst site, since its structure is very similar to the cocatalyst, and can therefore, interact with the catalyst. Such a new complex (CAT/CTA) may have different comonomer selectivity, as it has been witnessed in our experimental data.

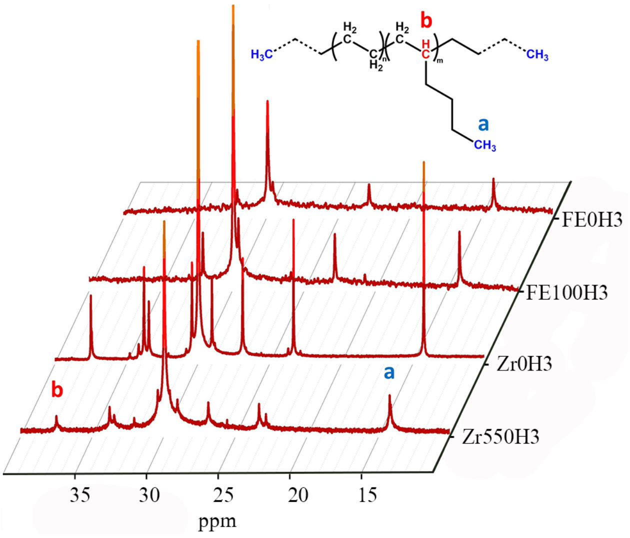

Figure 5. Effect of CTA on the ^{13}C NMR spectra of copolymers made by the Zr and Fe catalysts with and without CTA.

CONCLUSION

Designing new products based on CCTP reaction, like novel OBCs or chain-end functional polyolefins, is not possible unless understanding the exact effect of the reversible transfer reaction on the catalyst performance and the microstructural features of the product. The current kinetic models for such reactions are controversially developed based on the individual performance of the catalysts, in the absence of CTA. We have investigated the effect of CTA on the copolymerization of ethylene and 1–hexene using two catalysts with drastically different comonomer selectivities. Our results confirm that, despite not all chains find the chance to experience the reversible transfer reaction; CTA has a significant effect on the catalyst performance. For the case of the utilized metallocene catalyst, the activity is twice and the comonomer selectivity is about 30% lower, in presence of CTA. While, at the same reaction conditions, the activity of the selected late transition metal catalyst decreases and the comonomer selectivity does not change. Consequently, there is interplay between the reversible transfer of growing chains and the catalyst performance specifically in terms of comonomer incorporation. Specifically, the steric hindrance due to the frequent complexation of CTA seems to affect the incorporation of bulkier monomer to a greater extent. These results provide guidelines to correct the current approaches for modeling CCTP reaction, specifically using the binary catalytic systems. However, the obtained results, specifically the MMDs and activities, demonstrate that, at the reaction temperature that the performance of the utilized catalysts may match, their simultaneous application may not provide a useful OBC.

ACKNOWLEDGMENT

MA is a Georg Forster fellow of the Alexander von Humboldt Foundation and gratefully acknowledges this support.

REFERENCES

1. Domski GJ, Rose JM, Coates GW, Bolig AD, Brookhart M (2007) Living alkene polymerization: New methods for the precision synthesis of polyolefins. Prog polym Sci 32: 30-92
2. Makio H, Terao H, Iwashita A, Fujita T (2011) FI catalysts for olefin polymerization- A comprehensive treatment. Chem Rev 111: 2363-2449
3. Rouholahnejad F, Mathis D, Chen P (2009) Narrowly distributed polyethylene via reversible chain transfer to aluminum by a sterically hindered zirconocene/MAO. Organometallics 29: 294-302
4. Valente A, Mortreux A, Visseaux M, Zinck P (2013) Coordinative chain transfer polymerization. Chem Rev 113: 3836-3857
5. Britovsek GJ, Cohen SA, Gibson VC, Maddox PJ, van Meurs M (2002) Iron-catalyzed polyethylene chain growth on zinc: Linear α-olefins with a Poisson distribution. Angew Chem Int Ed 41: 489-491
6. Britovsek G, Cohen SA, Gibson VC, van Meurs M (2004) Iron catalyzed polyethylene chain growth on zinc: A study of the factors delineating chain transfer versus catalyzed chain growth in zinc and related metal alkyl systems. J Am Chem Soc 126: 10701-10712
7. Arriola DJ, Carnahan EM, Hustad PD, Kuhlman RL, Wenzel TT (2006) Catalytic production of olefin block copolymers via chain shuttling polymerization. Science 312: 714-719
8. Auriemma F, De Rosa C, Scoti M, Di Girolamo R, Malafronte A, D’Alterio MC, Boggioni L, Losio S, Boccia AC, Tritto I (2019) Structure and mechanical properties of ethylene/1-octene multiblock copolymers from chain shuttling technology. Macromolecules:DOI:10.1021/acs.macromol.8b02470
9. Ahmadi M, Saeb MR, Mohammadi Y, Khorasani MM, Stadler FJ (2015) A perspective on modeling and characterization of transformations in the blocky nature of olefin block copolymers. Ind Eng Chem Res 54: 8867-8873
10. Mohammadi Y, Ahmadi M, Saeb MR, Khorasani MM, Yang P, Stadler FJ (2014) A detailed model on kinetics and microstructure evolution during copolymerization of ethylene and 1-octene: From coordinative chain transfer to chain shuttling polymerization. Macromolecules 47: 4778-4789
11. Saeb MR, Khorasani MM, Ahmadi M, Mohammadi Y, Stadler FJ (2015) A unified picture of hard-soft segmental development along olefin chain shuttling copolymerization. Polymer 76: 245-253
12. Shan CLP, Hazlitt LG (2007) Block index for characterizing olefin block copolymers. Macromol Symp 257: 80-93
13. Wang H, Khariwala D, Cheung W, Chum S, Hiltner A, Baer E (2007) Characterization of some new olefinic block copolymers. Macromolecules 40: 2852-2862
14. Briquel R, Mazzolini J, Le Bris T, Boyron O, Boisson F, Delolme F, D'Agosto F, Boisson C, Spitz R (2008) Polyethylene building blocks by catalyzed chain growth and efficient end functionalization strategies, including click chemistry. Angew Chem Int Ed 47: 9311-9313
15. German I, Kelhifi W, Norsic S, Boisson C, D'Agosto F (2013) Telechelic polyethylene from catalyzed chain-growth polymerization. Angew Chem Int Ed 52: 3438-3441
16. Mazzolini J, Espinosa E, D'Agosto F, Boisson C (2010), Catalyzed chain growth (CCG) on a main group metal: an efficient tool to functionalize polyethylene. Polym Chem 1: 793-800
17. van Meurs M, Britovsek GJ, Gibson VC, Cohen SA (2005) Polyethylene chain growth on zinc catalyzed by olefin polymerization catalysts: Acomparative investigation of highly active catalyst systems across the transition series. J Am Chem Soc 127: 9913-9923
18. Kuhlman RL, Wenzel TT (2008) Investigations of chain shuttling olefin polymerization using deuterium labeling. Macromolecules 41: 4090-4094
19. Kuhlman RL, Klosin J (2010) Tuning block compositions of polyethylene multi-block copolymers by catalyst selection. Macromolecules 43: 7903-7904
20. Zinck P (2016) Unexpected reactivities in chain shuttling copolymerizations. Polym Int 65: 11-15
21. Boggioni L, Sidari D, Losio S, Stehling UM, Auriemma F, Di Girolamo R, De Rosa C, Tritto I

(2018) Ethylene–co–norbornene copolymerization in the presence of a chain transfer agent. Eur Polym J 107: 54-66

22. Boggioni L, Sidari D, Losio S, Stehling UM, Auriemma F, Malafronte A, Di Girolamo R, De Rosa C, Tritto I (2019) Ethylene-co-norbornene copolymerization using a dual catalyst system in the presence of a chain transfer agent. Polymers 11: 554
23. Vittoria A, Busico V, Cannavacciuolo FD, Cipullo R (2018) Molecular kinetic study of "chain shuttling" olefin copolymerization. ACS Catal 8: 5051-5061
24. Zhang M, Karjala TW, Jain P (2010) Modeling of α-olefin copolymerization with chain-shuttling chemistry using dual catalysts in stirred-tank reactors: Molecular weight distributions and copolymer composition. Ind Eng Chem Res 49: 8135-8146
25. Ahmadi M, Nasresfahani A (2015) Realistic representation of kinetics and microstructure development during chain shuttling polymerization of olefin block copolymers. Macromol Theor Simul 24: 311-321
26. Jandaghian MH, Soleimannezhad A, Ahmadjo S, Mortazavi SMM, Ahmadi M (2018) Synthesis and characterization of isotactic poly (1-hexene)/branched polyethylene multiblock copolymer via chain shuttling polymerization technique. Ind Eng Chem Res 57: 4807-4814
27. Hustad PD, Kuhlman RL, Carnahan EM, Wenzel TT, Arriola DJ (2008) An exploration of the effects of reversibility in chain transfer to metal in olefin polymerization. Macromolecules 41: 4081-4089
28. Zhang M, Carnahan EM, Karjala TW, Jain P (2009) Theoretical analysis of the copolymer composition equation in chain shuttling copolymerization. Macromolecules 42: 8013-8016
29. Zhang M, Karjala TW, Jain P, Villa C (2013) Theoretical modeling of average block structure in chain-shuttling α–olefin copolymerization using dual catalysts. Macromolecules 46: 4847-4853
30. Ribeiro R, Ruivo R, Nsiri H, Norsic SB, D'Agosto F, Perrin L, Boisson C (2016) Deciphering the mechanism of coordinative chain transfer polymerization of ethylene using neodymocene catalysts and dialkylmagnesium. ACS Catal 6: 851-860
31. Bhriain NN, Brintzinger H-H, Ruchatz D, Fink G (2005) Polymeryl exchange between a nsa-zirconocene catalysts for norbornene− ethene copolymerization and aluminum or zinc alkyls. Macromolecules 38: 2056-2063
32. Georges SB, Touré AO, Visseaux M, Zinck P (2014) Coordinative chain transfer copolymerization and terpolymerization of conjugated dienes. Macromolecules 47: 4538-4547
33. Loughmari S, Hafid A, Bouazza A, El Bouadili A, Zinck P, Visseaux M (2012) Highly stereoselective coordination polymerization of β-myrcene from a lanthanide-based catalyst: Access to biosourced elastomers. J Polym Sci Pol Chem 50: 2898-2905
34. Ventura A, Chenal T, Bria M, Bonnet F, Zinck P, Ngono-Ravache Y, Balanzat E, Visseaux M (2013) Trans-stereospecific polymerization of butadiene and random copolymerization with styrene using borohydrido neodymium/magnesium dialkyl catalysts. Eur Polym J 49: 4130-4140
35. Valente A, Zinck P, Mortreux A, Visseaux M (2009) Catalytic chain transfer (co-) polymerization: Unprecedented polyisoprene CCG and a new concept to tune the composition of a statistical copolymer. Macromol Rapid Commun 30: 528-531
36. Valente A, Stoclet G, Bonnet F, Mortreux A, Visseaux M, Zinck P (2014) Isoprene–styrene chain shuttling copolymerization mediated by a lanthanide half-sandwich complex and a lanthanidocene: straightforward access to a new type of thermoplastic elastomers. Angew Chem Int Ed 53: 4638-4641
37. Mahdavi H, Badiei A, Zohuri GH, Rezaee A, Jamjah R, Ahmadjo S (2007) Homogeneous polymerization of ethylene using an iron-based metal catalyst system. J Appl Polym Sci 103: 1517-1522
38. Xiao A, Wang L, Liu Q, Yu H, Wang J, Huo J, Tan Q, Ding J, Ding W, Amin AM (2009) A novel linear− hyperbranched multiblock polyethylene produced from ethylene monomer alone via chain walking and chain shuttling polymeriza-

tion. Macromolecules 42: 1834-1837

39. Mehdiabadi S, Soares JB (2016) Quantifying the copolymerization kinetics of ethylene and 1-octene catalyzed with rac-Et $(Ind)_2ZrCl_2$ in a solution reactor. Macromolecules 49: 2448-2457
40. Gibson VC, Redshaw C, Solan GA (2007) Bis (imino) pyridines: surprisingly reactive ligands and a gateway to new families of catalysts. Chem Rev 107: 1745-1776
41. Bianchini C, Giambastiani G, Rios IG, Mantovani G, Meli A, Segarra AM (2006) Ethylene oligomerization, homopolymerization and copolymerization by iron and cobalt catalysts with 2, 6-(bis-organylimino) pyridyl ligands. Coordination Chem Rev 250: 1391-1418
42. Tong Z-Z, Zhou B, Huang J, Xu J-T, Fan Z-Q (2014) Regulation of crystallization kinetics, morphology, and mechanical properties of olefinic blocky copolymers. Macromolecules 47: 333-346
43. Britovsek GJ, Gibson VC, McTavish SJ, Solan GA, White AJ, Williams DJ, Kimberley BS, Maddox PJ (1998) Novel olefin polymerization catalysts based on iron and cobalt. Chemical Communications 1998: 849-850
44. Ahmadi M, Rezaei F, Mortazavi SMM, Entezam M, Stadler FJ (2017) Complex interplay of short-and long-chain branching on thermal and rheological properties of ethylene/α-olefin copolymers made by metallocene catalysts with oscillating ligand structure. Polymer 112: 43-52
45. Awudza JA, Tait PJ (2008) The “comonomer effect” in ethylene/α-olefin copolymerization using homogeneous and silica-supported Cp_2ZrCl_2/MAO catalyst systems: Some insights from the kinetics of polymerization, active center studies, and polymerization temperature. J Polym Sci Pol Chem 46: 267-277
46. Ahmadi M, Nekoomanesh M, Jamjah R, Zohuri G Arabi H (2007) Modeling of slurry polymerization of ethylene using a soluble Cp_2ZrCl_2/MAO catalytic system. Macromol Theory Simul 16: 557-565
47. Wang W (2015) Effect of diethylzinc on the activity of ethylene polymerization by metallocene catalyst. Macromol React Eng 9: 333-338
48. Ahmadi M, Mortazavi SMM, Ahmadjo S, Zahmati M, Valieghbal K, Jafarifar D, Rashedi R (2016) Evaluation of continuous and discrete melting endotherms in determination of structural heterogeneities in Ziegler-Natta catalyzed linear low density polyethylene. Polyolefins J 3: 135-146
49. Hosoda S (1988) Structural distribution of linear low-density polyethylenes. Polym J 20: 383-397
50. Britovsek GJ, Clentsmith GK, Gibson VC, Goodgame DM, McTavish SJ, Pankhurst QA (2002) The nature of the active site in bis (imino) pyridine iron ethylene polymerisation catalysts. Catal Commun 3: 207-211
51. Liu W, Wang W-J, Fan H, Yu L, Li B-G, Zhu S (2014) Structure analysis of ethylene/1-octene copolymers synthesized from living coordination polymerization. Europ Polym J 54: 160-171
52. Mortazavi M, Arabi H, Zohuri GH, Ahmadjo S, Nekoomanesh M, Ahmadi M (2009) Ethylene homo-and copolymerization using a bis-IndZrCl2 metallocene catalyst: Structural composition distribution of the copolymer. Macromol React Eng 3: 263-270
53. Mortazavi SMM, Arabi H, Zohuri G, Ahmadjo S, Nekoomanesh M, Ahmadi M (2010) Copolymerization of ethylene/α-olefins using bis (2-phenylindenyl) zirconium dichloride metallocene catalyst: structural study of comonomer distribution. Polym Int 59: 1258-1265
54. Kissin YV, Qian C, Xie G, Chen Y (2006) Multicenter nature of ethylene polymerization catalysts based on 2, 6-bis (imino) pyridyl complexes of iron and cobalt. J Polym Sci Polym Chem 44: 6159-6170